Supporting Information for

Insights on the work function of the current collector surface in anode-free lithium metal batteries

Jinkwan Jung,‡[a] Ju Ye Kim,‡[acd] Il Ju Kim,[a] Hyeokjin Kwon,[a] Gukbo Kim,[ac] Gisu Doo,[a] Wonhee Jo,[a] Hee-Tae Jung*[ac] and Hee-Tak Kim*[ab]

[a] Department of Chemical and Biomolecular Engineering, Korea Advanced Institute of Science and Technology (KAIST), Daejeon 34141, Republic of Korea

[b] Advanced Battery Center, KAIST Institute for the NanoCentury, Korea Advanced Institute of Science and Technology, 335 Gwahangno, Yuseong-gu, Daejeon 34141, Republic of Korea

[c] Korea Advanced Institute of Science and Technology (KAIST) institute for NanoCentury, 291 Daehak-ro, Yuseong-gu, Daejeon 34141, Korea

[d] Brown University, School of Engineering, 184 Hope Street, Providence, RI 02912 USA.

‡ These authors contributed equally to this work.

*Corresponding author: E-mail: heetak.kim@kaist.ac.kr (H.-T. Kim); heetae@kaist.ac.kr (H.-T. Jung)

Supporting Figures

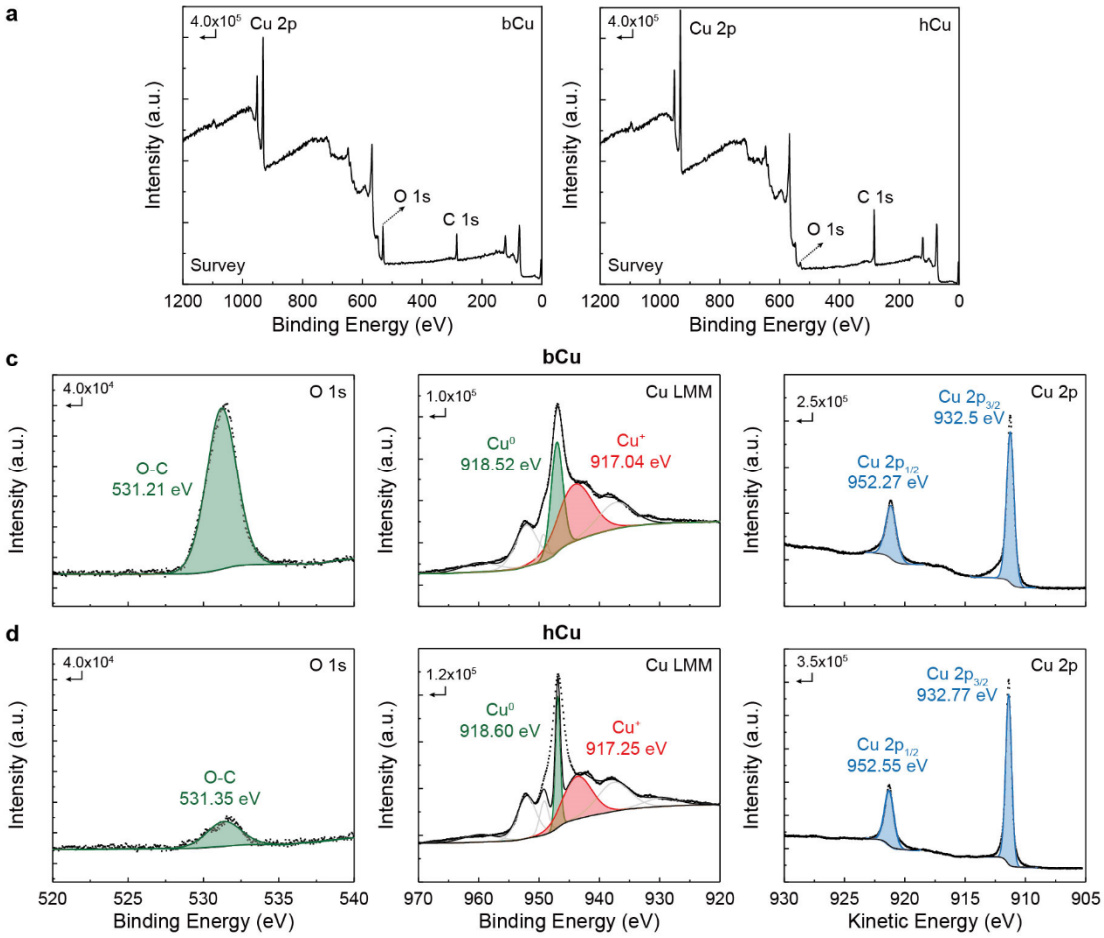

Fig. S1 Surface composition analysis using X-ray photoelectron spectroscopy (XPS). (a) Survey peak analysis for bCu and hCu. (b) O *1s*, Cu *LMM*, and Cu *2p* XPS spectra for bCu (top) and hCu (bottom).

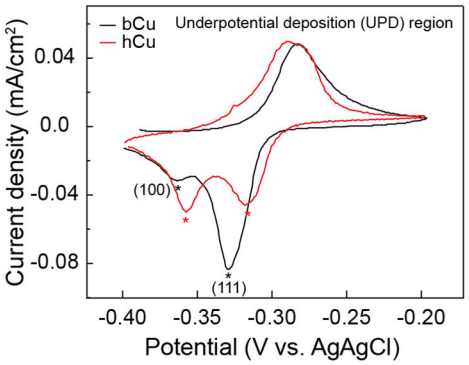

Fig. S2 Cyclic voltammograms for hCu and bCu film in 0.1 M $HClO_4$ + 1 mM $Pb(Cl)_2$ at a scan rate of 10 mV/s in a voltage range from -0.2 V to -0.4 V (vs. Ag/AgCl).

	bCu	hCu
Conductivity [S cm^{-1}]	9.68×10^{5}	1.26×10^{6}
R [ohm sq^{-1}]	1.2×10^{-4}	7×10^{-5}

Table. S1 Electrical surface conductivity and resistance of bCu and hCu measured using 4-point probe method.

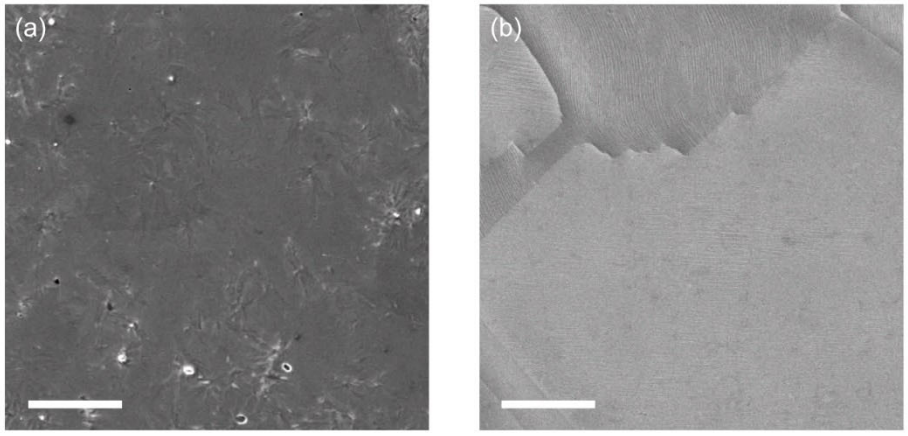

Fig. S3 Surface morphology of the Cu current collector surfaces. SEM images of (a) bCu and (b) hCu surface. Scale bars; 5 μm.

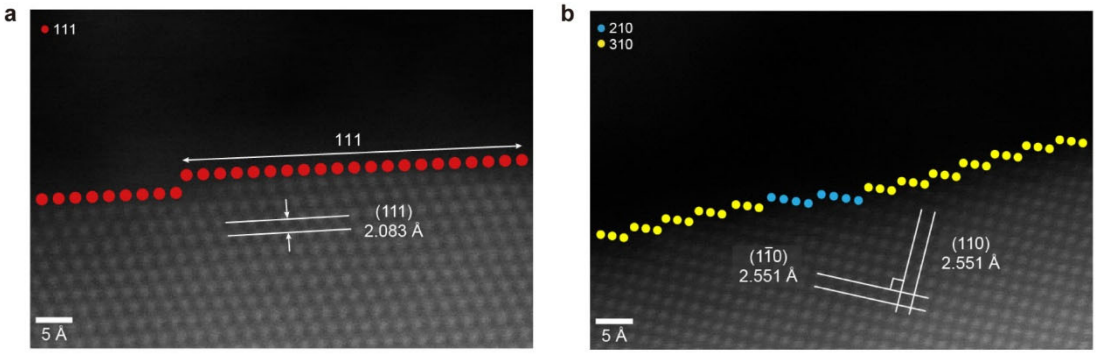

Fig. S4 Surface structure of Cu current collector after 10 cycles operation. TEM analysis for (a) bCu and (b) hCu after the repeated Li plating/stripping under 1 mA cm^{-2} / 1 mAh cm^{-2} condition for 10 cycles.

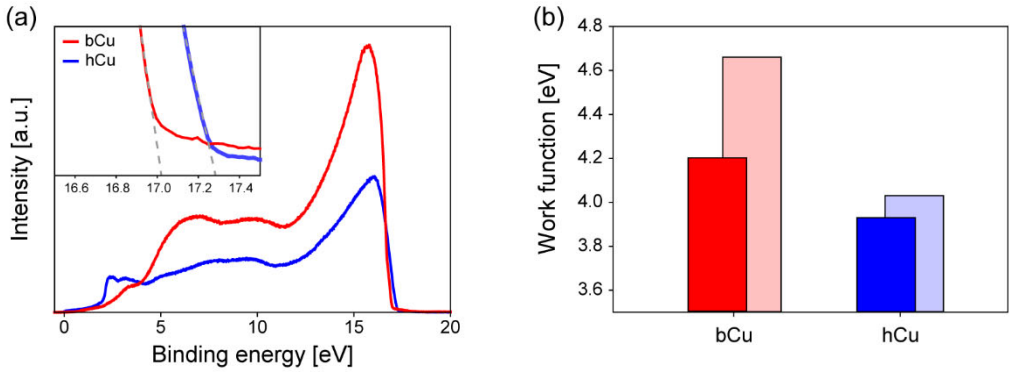

Fig. S5 Work function analysis for the Cu current collectors. (a) UPS analysis results for the bCu and hCu current collectors. (Inset: UPS spectra of the cut-off region) (b) Work functions of bCu and hCu current collectors investigated by UPS analysis and DFT simulation. Dark color and pale color indicate the work function obtained by each UPS analysis and DFT simulation.

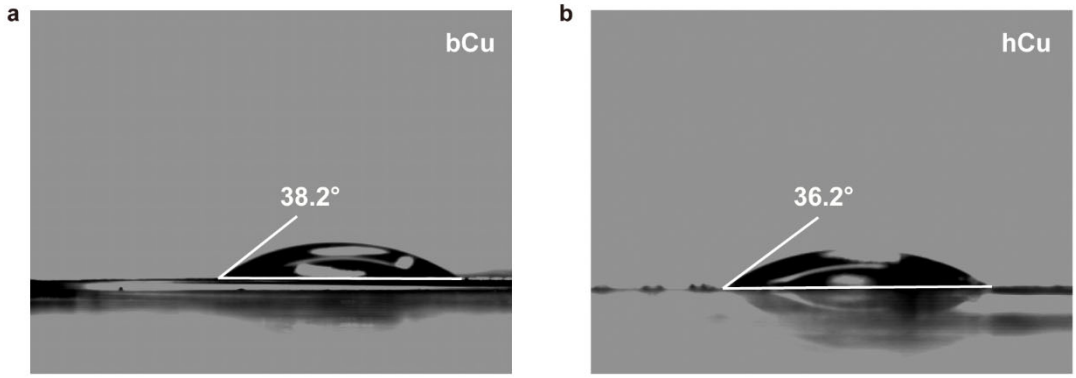

Fig. S6 Electrolyte wetting ability of bCu and hCu. Contact angle of the electrolyte drop (1 M LiFSI DME) on (a) bCu and (b) hCu.

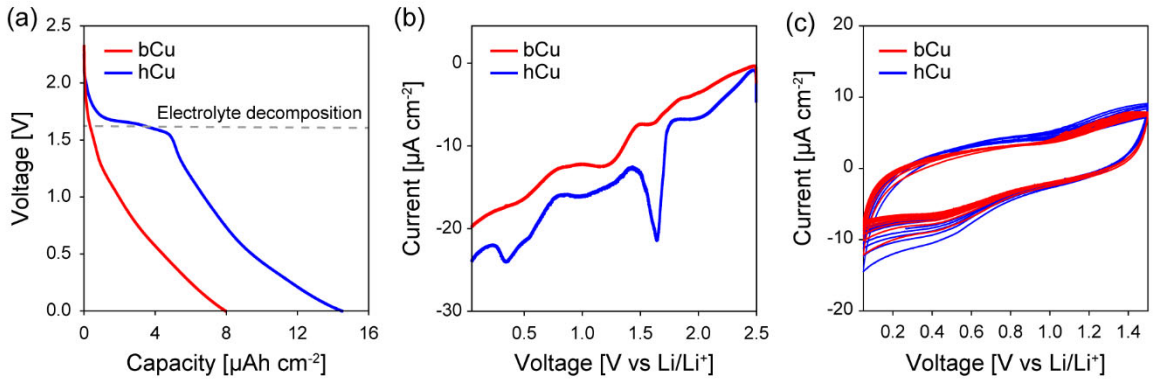

Fig. S7 Electrochemical analysis of the electrolyte decomposition on the current collector surface. (a) Galvanostatic reduction at 0.05 mA cm^{-2}, (b) linear sweep voltammetry analysis at a sweep rate of 1 mV s^{-1}, and (c) 10 cycles of cyclic voltammetry at a scan rate of 1 mV s^{-1} in the range of 0.05 to 1.5 V voltage range for bCu and hCu current collector.

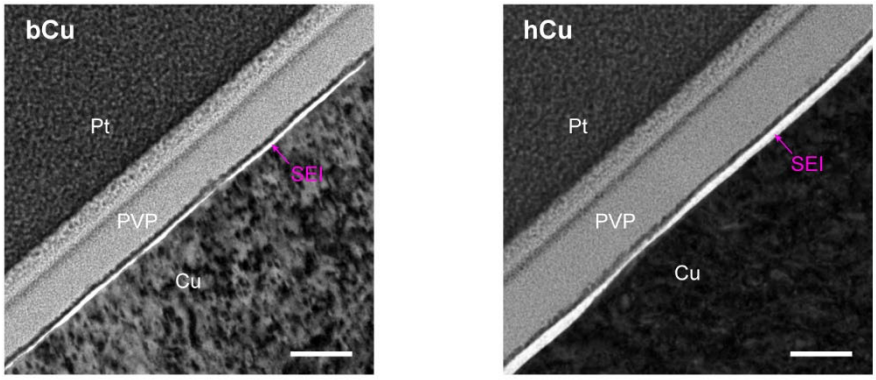

Fig. S8 Low magnification TEM images of the cross-section of bCu and hCu after the CV cycling (Fig. S7). Scale bars; 100 nm.